JASA Express Letters

NOVEMBER 07 2024

An experimental approach for comparing the influence of cello string type on bowed attack response

Alessio Lampis ; Alexander Mayer; Vasileios Chatziioannou

JASA Express Lett. 4, 113201 (2024)
https://doi.org/10.1121/10.0034330

JASA EXPRESS LETTERS ARTICLE asa.scitation.org/journal/jel

An experimental approach for comparing the influence of cello string type on bowed attack response

Alessio Lampis,[a] **Alexander Mayer, and Vasileios Chatziioannou**
Departments of Music Acoustics–Institut für Wiener Klangstil, University of Music and Performing Arts Vienna, Vienna, 1030, Austria
lampis@mdw.ac.at, mayer@mdw.ac.at, chatziioannou@mdw.ac.at

Abstract: This study investigates the influence of string properties on bowed string attack playability. To assess the attack playability of different string types, a variety of bow forces and bow accelerations were chosen to excite the strings and measure the transient response under different bowing control parameters. The experimentally obtained playability maps of transient duration as function of bow force and acceleration (Guettler diagram) were obtained with a robotic bowing machine, from four different types of cello G2 strings. Results indicate variations in playability across string types, suggesting that string properties impact attack duration.

[Editor: D Murray Campbell] https://doi.org/10.1121/10.0034330

Received: 26 August 2024 **Accepted:** 24 October 2024 **Published Online:** 7 November 2024

1. Introduction

Playability in bowed string instruments is often assessed through bowing parameter diagrams, which predict how such parameters (e.g., bow force, speed, bowing position) influence sound production. These diagrams, also called playability maps, define regions where notes are easily playable or where specific string oscillations occur. While Schelleng diagrams consider steady-state interactions (Schelleng, 1973), the Guettler diagram shows the transient duration as a function of bowing parameters, in order to represent how fast Helmholtz motion is achieved during an attack (Guettler, 2002). Specifically, it indicates how musicians could adjust bow force and bow acceleration to control transient responses. According to Guettler's analysis, the area in such a diagram where the string plays with a "perfect attack" forms a triangular region, with the vertex pointing towards the origin. Experimental assessments of the transient response show deviations from this triangular region (Galluzzo *et al.*, 2017; Lampis *et al.*, 2024). Guettler diagrams can be constructed based on simplified analytical solutions (Guettler, 2002) or populated using experimental data (Galluzzo and Woodhouse, 2014; Lampis *et al.*, 2024) or numerical simulations (Galluzzo *et al.*, 2017; Mansour *et al.*, 2016b; Matusiak and Chatziioannou, 2024). It has to be pointed out that transient phenomena remain in a certain extent unclear, as a physical model that accurately describes the friction forces between the bow and the string has not been found yet, even if latest efforts seem promising (euphonics.org, 2024; Matusiak and Chatziioannou, 2024).

String manufacturers offer a wide variety of strings to enhance loudness and tone control, also thanks to the advancements in string technology and material selection, and musicians invest significant time in choosing strings based on playing style and instrument type. Extensive experimental investigations have been carried out regarding the string properties role on tonal features of bowed strings (Pickering, 1990) and some on transient behaviour (Pickering, 1986). Current research suggests minimal influence of strings on perceived playability (Fu *et al.*, 2018). The role of strings in playability remains unclear, with evaluations often relying on subjective musician preferences.

This study proposes a systematic approach to address this gap. We employ a bowing machine to measure the transient response of different string types. The resulting data is used to create Guettler diagrams in order to show how string characteristics affect attack playability.

2. Experiment

A custom-designed monochord is used to measure bowing parameters and string response during transient attacks (Mayer and Lampis, 2024). A bowing machine, consisting of a robotic arm, excites the strings with a range of bow forces $F_b = 1.15 - 3.5\,\mathrm{N}$ and accelerations $a = 0.15 - 3.15\,\mathrm{ms}^{-2}$ commonly used by musicians. String vibrations are measured by a sensing bridge capturing the force exerted on the termination of the string (Lampis *et al.*, 2023). The robotic arm controls the bow. The bow force is measured by load cells between the bow and the arm. The bow moves in linear

[a]Author to whom correspondence should be addressed.

motions perpendicular to the string. The robotic arm's movement, along with bow and bridge force signals, are recorded for retrieving the bowing parameters. A dedicated technical report (Mayer and Lampis, 2024) provides a more detailed description of the apparatus, while a previous study contains the procedure for obtaining Guettler diagrams with this setup (Lampis *et al.*, 2024).

Each string type (A, B, C, D)—all commercially available G2 cello strings—was excited with various bow strokes at constant bow force and acceleration. Initial bow stroke velocity was zero, and the bowing position was fixed at $x_{\text{bow}} = 5.5\,\text{cm}$ from the bridge. With a playing length of $L = 70\,\text{cm}$, the relative bow-bridge distance $\beta = x_{\text{bow}}/L$ was $\beta = 0.0786$. To account for string settling and known transient chaotic behaviour (Galluzzo *et al.*, 2017), six Guettler diagrams were measured for each string. Four were obtained consecutively, reversing the measurement order each time. The remaining two were measured after dismounting and remounting the string one month later. The reversing of order accounts for the fresh rosin applied at the beginning of each repetition.

We measured basic string properties related to transverse behaviour. Additionally, string brand and type are listed below:

String A: D'Addario Prelude.	String C: Thomastik Infeldt Dominant Cello.
String B: D'Addario Helicore.	String D: D'Addario Kaplan.

Other information regarding technological processes for string making is unavailable, due to manufacturer confidentiality.

2.1 String properties of different types

String properties related to transverse vibration were measured directly on the monochord, ensuring that these characteristics reflect the state of the string during bowing. We used a caliper to measure the diameter d, and a load cell embedded in the apparatus to measure tension T. Linear density μ and transverse impedance Z were calculated using the following formulas: $\mu = T/(2Lf_0)^2$, $Z = \sqrt{\mu T}$ (f_0 is the fundamental frequency measured from the string's pluck response).

String properties were measured repeatedly throughout the experiment, before and after acquiring the data for each Guettler diagram. The string's pluck response, measured at the same bowing position x_{bow} using the breaking-wire method, was used to estimate some string properties. We performed 12–15 plucks per string to account for slight properties variations that occurred since the string was not tuned during each Guettler diagram measurement.

Inharmonic spacing of natural frequencies f_n is used to estimate the bending stiffness B. The theoretical quadratic relationship between the normalized natural frequency f_n/n and mode number n is expressed as $f_n/n \approx f_0 + \gamma n^2$, with $B \approx (2\gamma TL^2)/(f_0\pi^2)$ (Lynch-Aird and Woodhouse, 2017). We obtained B by fitting this equation to the measured normalized frequencies (see Fig. 1, right plot). Data points with a z-score (the absolute value of the fitting residual, normalized by its standard deviation) greater than 3 were excluded to ensure a better quadratic fit.

The pluck response also provided an estimate of the quality factor Q as a function of frequency. We computed the slope of the decay response for each natural frequency (first 30 modes) of the logarithmically scaled, filtered signal (bandpass Butterworth filter: $\pm 20\,\text{Hz}$ around the natural frequency). Fits with a correlation coefficient $R^2 < 0.98$ were excluded. Figure 1 (left plot) shows the Q factors as a function of mode number, along with the best fit of the Valette model for frequency-dependent damping (Valette, 1995) using the expression in Mansour *et al.* (2016a). The averaged Q factor across modes $\hat{Q}$, and the average and standard deviation of the other string properties are reported in Table 1.

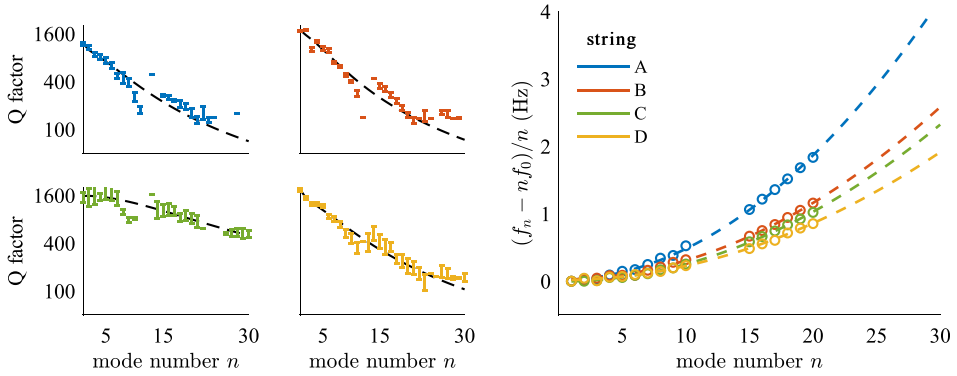

Fig. 1. Left: Q factors of the four string types as a function of mode number for the first 30 modes. Right: For the same modes and string types, the normalized natural frequency deviation as a function of mode number for indicating the inharmonicity of each type.

Table 1. Main transversal string properties of the four cello G string types under investigation.

String	d (mm)	T (N)	μ (g/m)	Z (kg/s)	B (10^{-4} N m^2)	$\hat{Q}$ (—)
A	1.092	149.6 ± 1.3	7.94 ± 0.07	1.09 ± 0.01	6.85 ± 0.14	419
B	0.877	153.2 ± 0.8	8.14 ± 0.03	1.12 ± 0.005	4.32 ± 0.16	503
C	1.15	116.3 ± 0.7	6.2 ± 0.06	0.85 ± 0.007	3.03 ± 0.07	1064
D	0.895	153.5 ± 0.9	8.2 ± 0.04	1.13 ± 0.005	3.1 ± 0.42	521

3. Attack playability

Bridge force signals were used to assess attack playability as a function of bowing parameters. We employed an automatic waveform identification algorithm (Galluzzo, 2004) to compute the duration between the initial slip (right after the limiting static friction is reached) and the establishment of stable Helmholtz motion [details in Lampis *et al.* (2024)].

Figure 2 (left) presents an example of a Guettler diagram for one string, with transient duration plotted as scatter data against bow force and acceleration and colour coded between 0 and 20 periods. We arbitrarily chose to display transient durations up to 20 string fundamental periods, following previous works (Galluzzo, 2004), and considered these successful attacks. While 20 periods correspond to roughly 0.2 s, exceeding typical player expectations for an acceptable attack (Guettler and Askenfelt, 1997), including longer durations improves visualization of a playable region within the Guettler diagram. Four waveforms from this diagram are shown on the right side of Fig. 2, as examples. These bridge force signals have different transient durations, ranging from a "perfect attack" (0 periods) to an attack exceeding 20 periods (unsuccessful attack).

3.1 Analysis of playability limits

The boundaries of the playable region in Fig. 2 (left) resemble straight lines, as expected by Guettler's conditions (Guettler, 2002). These boundaries can be interpreted as the playable limits for bow force and acceleration. However, closer examination reveals small deviations from perfectly straight boundaries. This is partly due to the non-uniform distribution of the measured data points and partly due to the inherently chaotic nature of bowed transients (Galluzzo *et al.*, 2017). Consequently, some non-playable data points (black) appear within the playable region, even near "perfect attacks." This speckled pattern is particularly evident near the transition between playable and non-playable zones.

To quantify attack playability for each string type, we fit two lines to the boundaries of the playable region in the Guettler diagram (Fig. 2, left). The left and right data points of the borders are identified first, followed by fitting linear equations to them, of the form $F_L = c_L a + k_L$ and $F_R = c_R a + k_R$, where a represents bow acceleration. The slopes (c_L and c_R) of these lines provide an initial indication of the acceleration range for achieving successful attacks. While for higher c_L the raucous motion region (on the left of F_L) decreases, a higher c_R suggests a more critical limitation in acceleration before falling into the multiple slips motion region (on the right of F_R).

We then calculate the percentage p of successful transients within the playable region. This percentage reflects the prevalence of "dark" data points within the playable region, indicating the intensity of the chaotic transient behaviour. Additionally, we measure the average transient duration $\hat{t}$ of successful attacks and the area A_p of the playable region, obtained from the linear fits.

3.2 Comparison of different string types

Figure 3 shows the Guettler diagrams for all four string types. The first four repetitions were performed consecutively, and the last two measured one month later. Repetitions 2, 4, and 6 were conducted in reverse order to account for potential

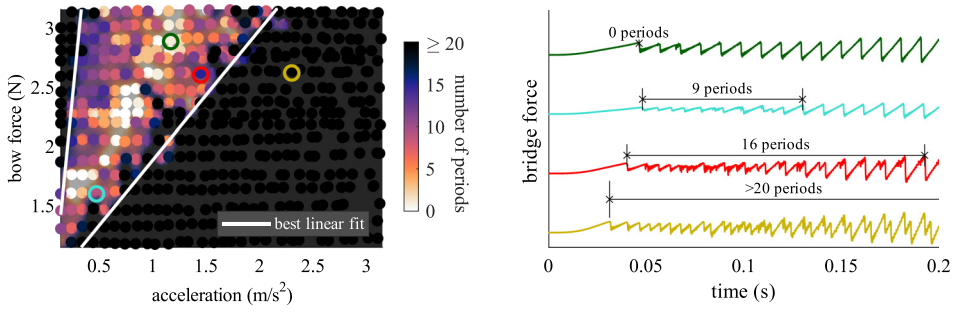

Fig. 2. Left: bow force–bow acceleration diagram displaying the transient time during attacks (Guettler diagram) including the best linear fit to the left and right playability limit. Right: bridge force signal for attacks (circles in the Guettler diagram) including the duration of the transient; from top to bottom: perfect attack, two successful attacks and a non-successful attack.

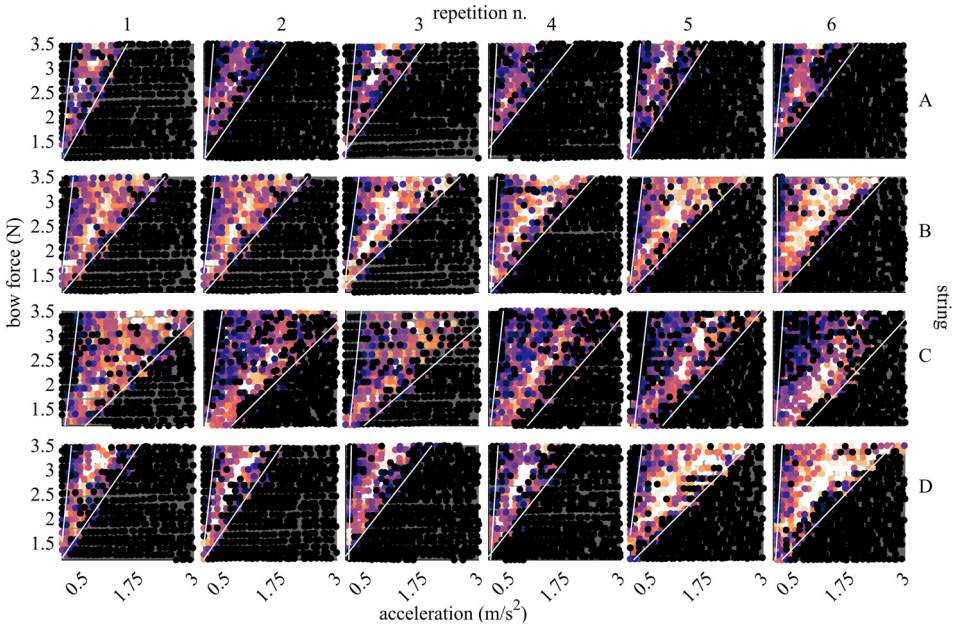

Fig. 3. Twenty-four Guettler diagrams for the four string types, arranged along the rows with the order of repetition. White lines represent the best fit to the boundaries of the playable region.

systematic effects. Visually inspecting the data (Fig. 3), we observe a high degree of repeatability in terms of size, shape, and duration of the playable regions for strings A, B, and C. Additionally, the differences between string types appear more pronounced than the differences between repeated measurements on the same string.

However, this consistency across repetitions does not hold for string D. After remounting the string, its playable region showed a significant increase in size. The right border shifted considerably downward, and the overall transient duration decreased. This suggests that remounting the string may have altered its properties, potentially influencing the playability.

Table 2 summarizes the playability features extracted from Fig. 3. String A has the lowest responsiveness, reflected by its small, sparsely populated playable region. It also has the highest c_R, the highest average transient duration $\hat{t}$, and smallest playable region area A_p. In contrast, string B displays the lowest c_L (biggest raucous region), the highest percentage of successful transients p, indicating greater stability within the playable region, and the shortest average transient duration $\hat{t}$. String C has the lowest p, suggesting a more chaotic transient behaviour due to the prevalence of unsuccessful transients within its playable region. Additionally, the borders of its playable region deviate from straight lines, especially when the measurement order is reversed. This behaviour points out the limitations of using straight lines for quantifying the playable area in cases like string C, as also shown by the high variability of most features. String D also exhibits high variability, primarily due to the last two repetitions after remounting the string.

Interestingly, the bending stiffness B of string D decreased by 29% after remounting. This change is considerably larger than the observed variations in other types after remounting (around 5%). While other properties of string D also changed after remounting, the magnitude of change remained within the range observed for other types. This change in the bending stiffness could partially explain the change in responsiveness of this string.

To provide a more intuitive view of the differences between string types, we computed the average transient duration across the first four repetitions. We did this by interpolating the scattered data points onto a regular grid (100×100 points) and then computing the mean value of the transient times across repetitions (Fig. 4, top row). These

Table 2. Playability features extracted from the Guettler diagrams of Fig. 3 for the four string types. The deviation indicates the variability across six repetitions.

String	c_L	k_L	c_R	k_R	p (%)	$\hat{t}$ (periods)	A_p
A	8.79 ± 3.3	-0.068 ± 0.9	1.4 ± 0.1	0.9 ± 0.1	71.39 ± 2.8	10.26 ± 0.3	1.74 ± 0.2
B	6.34 ± 4.7	0.46 ± 1.3	1.02 ± 0.1	0.93 ± 0.1	85.03 ± 3.2	6.74 ± 0.87	2.46 ± 0.2
C	6.74 ± 3.7	0.03 ± 0.9	1.17 ± 0.1	0.13 ± 0.47	70.68 ± 3.25	9 ± 0.65	3.71 ± 0.62
D	10.9 ± 4.1	-1.46 ± 2.8	1.13 ± 0.2	0.97 ± 0.1	77.63 ± 5.4	7.38 ± 1.3	2.28 ± 0.62

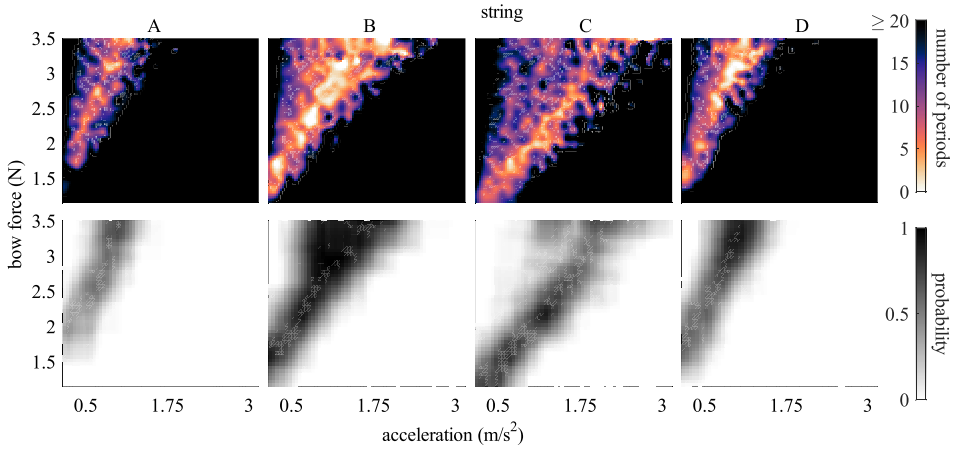

Fig. 4. Top: averaged transient time for each string type, obtained by computing the mean of the transient time on an interpolated grid across the first four Guettler diagrams. Bottom: probability map of the above Guettler diagrams of achieving a transient time shorter than 10 period lengths.

averaged Guettler diagrams accentuate areas with shorter transients. Interestingly, the speckled patterns observed in individual repetition of Guettler diagrams are partially mitigated in these averaged plots, particularly for strings A and B.

To further highlight areas of short transients, we calculated the probability of encountering a transient shorter than 10 periods (considered more "musically" acceptable) using a sliding window within the averaged Guettler diagrams (Fig. 4, bottom row) with dimension $0.5\,\mathrm{ms}^{-2} \times 0.5\,\mathrm{N}$ and steps of $0.05\,\mathrm{ms}^{-2} \times 0.5\,\mathrm{N}$. Musicians likely manipulate bowing parameters to stay within these high-probability regions, avoiding the speckled behaviour seen in individual diagrams. This suggests that certain string types, like string B with a broader high-probability area, may be easier to play due to a wider range of possible bowing parameters. In contrast, types with smaller probability maps, like string A, might require more precise manipulation of bow force and acceleration for achieving successful attacks.

4. Discussion

This study investigated the influence of string properties on attack playability using four commercially available G2 cello strings. We excited the strings with a robotic bowing machine for different bow forces and accelerations. Transient attack durations were measured and plotted as a function of the bowing parameters (Guettler diagrams), revealing playability regions for each string type. These regions differed in size, shape, and mean transient duration, suggesting differences in playability across strings. Interestingly, string B exhibited the fastest averaged transient duration, while string A was the least responsive. Remounting string D significantly altered its playability. It seems likely that this change can be explained by the appreciable variation in bending stiffness, that was observed when remounting the string. This aspect requires additional investigations, such as an analysis of the winding in the process of remounting the string.

Further studies are needed to better understand the influence of string properties on playability across a wider variety of string types and bowing parameters, as we limited the experiments to four string types and a single bowing position. Moreover, previous preliminary analysis (not reported here), where string properties were not measured, showed smaller differences in responsiveness between types than observed in this study. For this reason (among others) it would be highly desirable to expand the analysis to more samples from the same string type. Furthermore, the current setup did not measure torsional properties, which might play a crucial role in damping and responsiveness. Future investigations should consider these properties for a more comprehensive understanding.

To conclude, the observations of this study necessitate further investigations, ideally by measuring the actual bowing parameters used by experienced musicians during "perfect attacks" to confirm the hypothesized relation between string types and playability.

Acknowledgments

This research was funded in whole or in part by the Austrian Science Fund (FWF) [10.55776/P34852]. We would like to thank Fan Tao and Tom Nania (both at D'Addario & Co.) for providing the D'Addario strings for the experiments.

Author Declarations

Conflict of Interest

The authors have no conflicts to disclose.

Data Availability

The bridge force waveforms associated with this article are available in Zenodo with a Creative Commons Attribution 4.0 International licence, under the reference Lampis (2024). Other data relative to this study are available from the corresponding author upon reasonable request.

References

euphonics.org (**2024**). "Euphonics: The science of musical instruments, Chap. 9, Secs. 9.5 and 9.6" https://euphonics.org/9-5-getting-that-perfect-start-guettlers-diagram/ (Last viewed October 3, 2024).

Fu, L., Scavone, G., and Fritz, C. (**2018**). "How different strings affect violin qualities," Proc. Mtgs. Acoust. **35**(3), 035003.

Galluzzo, P. (**2004**). "On the playability of stringed instruments," Ph.D. thesis, University of Cambridge, Cambridge, UK.

Galluzzo, P., and Woodhouse, J. (**2014**). "High-performance bowing machine tests of bowed-string transients," Acta Acust. united Acust. **100**(1), 139–153.

Galluzzo, P., Woodhouse, J., and Mansour, H. (**2017**). "Assessing friction laws for simulating bowed-string motion," Acta Acust. united Acust. **103**(6), 1080–1099.

Guettler, K. (**2002**). "On the creation of the Helmholtz motion in bowed strings," Acta Acust. united Acust. **88**(6), 970–985.

Guettler, K., and Askenfelt, A. (**1997**). "Acceptance limits for the duration of pre-Helmholtz transients in bowed string attacks," J. Acoust. Soc. Am. **101**(5), 2903–2913.

Lampis, A. (**2024**). "Bridge force waveforms obtained by systematically bowing various cello G-string models [data set]," Zenodo. https://doi.org/10.5281/zenodo.13374477 (Last viewed October 31, 2024).

Lampis, A., Mayer, A., and Chatziioannou, V. (**2024**). "Assessing playability limits of bowed-string transients using experimental measurements," Acta Acust. **8**, 44.

Lampis, A., Mayer, A., Pàmies-Vilà, M., and Chatziioannou, V. (**2023**). "Examination of the static and dynamic forces at the termination of a bowed string," J. Acoust. Soc. Am. **153**(3), A198.

Lynch-Aird, N., and Woodhouse, J. (**2017**). "Mechanical properties of nylon harp strings," Materials **10**(5), 497.

Mansour, H., Woodhouse, J., and Scavone, G. P. (**2016a**). "Enhanced wave-based modelling of musical strings. Part 1: Plucked strings," Acta Acust. united Acust. **102**(6), 1082–1093.

Mansour, H., Woodhouse, J., and Scavone, G. P. (**2016b**). "Enhanced wave-based modelling of musical strings. Part 2: Bowed strings," Acta Acust. united Acust. **102**(6), 1094–1107.

Matusiak, E., and Chatziioannou, V. (**2024**). "Elasto-plastic friction modeling toward reconstructing measured bowed-string transients," J. Acoust. Soc. Am. **156**(2), 1135–1147.

Mayer, A., and Lampis, A. (**2024**). "A versatile monochord setup: An industrial robotic arm as bowing and plucking device," technical report.

Pickering, N. (**1990**). "String tone quality related to core material," Catgut Acoust. Soc. J. **1**(5), 23–28.

Pickering, N. C. (**1986**). "Transient response of certain violin strings," Catgut Acoust. Soc. J. **1**(45), 24–26.

Schelleng, J. (**1973**). "The bowed string and the player," J. Acoust. Soc. Am. **53**(1), 26–41.

Valette, C. (**1995**). "The mechanics of vibrating strings," in *Mechanics of Musical Instruments*, edited by A. Hirschberg, J. Kergomard, and G. Weinreich (Springer-Verlag, New York), Vol. 355, pp. 115–183.